Phase Evolution in Low-Dimensional Niobium Oxide Synthesized by a Topochemical Method

Lihong Li,[†] Jinxia Deng,[†] Ranbo Yu,[†] Jun Chen,[†] Xiaowei Wang,[†] and Xianran Xing*,[†,‡]

[†]*Department of Physical Chemistry and* [‡]*State Key Laboratory for Advanced Metals and Materials, University of Science and Technology Beijing, Beijing 100083, China*

In this paper, we report a catalyst-free topochemical method, combined with molten salt synthesis (MSS), to synthesize, on a large scale, rodlike and platelet single crystals of Nb_2O_5. Rodlike KNb_3O_8 and platelet $K_4Nb_6O_{17}$, which were fabricated as the precursors by the molten salt method, were treated by proton exchange and heat treatment to synthesize the rodlike $H-Nb_2O_5$ and platelet $T-Nb_2O_5$ single crystal, respectively. The synthesized niobium pentaoxides retained the rodlike and platelet shapes of their precursors. The structural changes involved in the process were investigated by Raman spectroscopy, X-ray diffraction, scanning electron microscopy, and transmission electron microscopy. A possible topochemical reaction mechanism is proposed. Furthermore, rodlike and platelet $KNbO_3$ powders were derived from stable $H-Nb_2O_5$ and $T-Nb_2O_5$, respectively.

Introduction

Low-dimensional structures of transition metal oxides have attracted great attention because of their unique shape-dependent properties, such as ferroelectricity,[1,2] piezoelectricity,[3−5] ferromagneticity,[6] and optical properties.[7] Many experimental efforts have been made to prepare tubes,[8−10] rods, and wires,[3,4,6,7,11−13] as well as sheets and platelets.[2,5,14,15] For example, ZnO wire was used as a mechanical-electrical trigger,[3] and TiO_2/SnO_2 tapes showed ferromagnetic properties at room temperature.[6] Moreover, materials of this type were used as templates (physical or chemical) to generate 1D and 2D structures of functional oxides[16] and could also be employed as seeds to form texture ceramics having high-performance piezoelectric properties.[2] Therefore, many synthetic methods, such as the hydrothermal method,[17] molten salt synthesis (MSS),[18] gas-phase synthesis,[19] and cold plasma treatment,[20] have been developed to synthesize anisotropic transition metal oxides with different shapes.

Niobates have considerable nonlinear optical, ferroelectric, piezoelectric, ionic conductive, pyroelectric, photorefractive, and photocatalytic properties.[21] Of these materials, Nb_2O_5 is one of the most important transition metal oxides, with promising application in electrochromism[22] and catalysis[23] as well as in field-emission displays[24] and microelectronics.[20] In addition, it is the favorite raw material of other niobates (such as $ANbO_3$ (A = Li, Na, K, etc.) and $M^IM^{II}Nb_3O_{10}$ (M^I = Li, Na, K, Rb, Cs, Tl; M^{II} = Ca)[25])

*To whom correspondence should be addressed. E-mail: xing@ustb.edu.cn.
(1) Yun, W. S.; Urban, J. J.; Gu, Q.; Park, H. *Nano Lett.* **2002**, *2*, 447–450.
(2) Saito, Y.; Takao, H.; Tani, T.; Nonoyama, T.; Takatori, K.; Homma, T.; Nagaya, T.; Nakamura, M. *Nature* **2004**, *432*, 84–87.
(3) Zhou, J.; Fei, P.; Gao, Y.; Gu, Y.; Liu, J.; Bao, G.; Wang, Z. L. *Nano Lett.* **2008**, *8*, 2725–2730.
(4) Suyal, G.; Colla, E.; Gysel, R.; Cantoni, M.; Setter, N. *Nano Lett.* **2004**, *4*, 1339–1342.
(5) Li, L.; Chen, J.; Deng, J.; Yu, R.; Qiao, L.; Liu, G.; Xing, X. *Eur. J. Inorg. Chem.* **2008**, *2008*, 2186–2190.
(6) He, R. R.; Law, M.; Fan, R.; Kim, F.; Yang, P. *Nano Lett.* **2002**, *2*, 1109–1013.
(7) Nakayama, Y. P.; Pauzauskie, P. J.; Radenovic, A; Onorato, R. M.; Saykally, R. J.; Liphardt, J.; Yang, P. D. *Nature* **2007**, *447*, 1098–1101.
(8) Tong, Z.; Takagi, S.; Shimada, T.; Tachibana, H.; Inoue, H. *J. Am. Chem. Soc.* **2006**, *128*, 684–865.
(9) Ma, R.; Bando, Y.; Sasaki, T. *J. Phys. Chem. B* **2004**, *108*, 2115–2119.
(10) Kobayashi, Y.; Hata, H.; Salama, M.; Mallouk, T. E. *Nano Lett.* **2007**, *7*, 2142–2145.
(11) Mozetic, M.; Cvelbar, U.; Sunkara, M. K.; Vaddiraju, S. *Adv. Mater.* **2005**, *17*, 2138–2142.
(12) Varghese, B.; Haur, S. C.; Lim, C. *J. Phys. Chem. C* **2008**, *112*, 10008–10012.
(13) Kumar, V.; Kim, J. H.; Pendyala, C.; Chernomordik, B.; Sunkara, M. K. *J. Phys. Chem. C* **2008**, *112*, 17750–17754.
(14) Wang, X.; Li, L.; Zhang, Y.; Wang, S.; Zhang, Z.; Fei, L.; Qian, Y. *Cryst. Growth Des.* **2006**, *6*, 2163–2165.
(15) Yang, H. G.; Zeng, H. C. *J. Phys. Chem. B* **2004**, *108*, 819–823.
(16) Xia, Y.; Yang, P.; Sun, Y.; Wu, Y.; Mayers, B.; Gates, B.; Yin, Y.; Kim, F.; Yan, H. *Adv. Mater.* **2003**, *15*, 353–389.
(17) Wang, Z. *J. Nanosci. Nanotechnol.* **2007**, *8*, 27–55.
(18) Kong, X.; Sun, X.; Li, Y. *Chem. Lett.* **2003**, *32*, 546–547.
(19) Kumar, V.; Kim, J. H.; Pendyala, C.; Chernomordik, B.; Sunkara, M.; K. *J. Phys. Chem. C* **2008**, *112*, 17750–17754.
(20) Mozetic, M.; Cvelbar, U.; Sunkara, M. K.; Vaddiraju, S. *Adv. Mater.* **2005**, *17*, 2138–2142.
(21) Guo, Y.; Kakimoto, K.; Ohsato, H. *Appl. Phys. Lett.* **2004**, *85*, 4121.
(22) Ozer, N.; Chen, D. G.; Lampert, C. M. *Thin Solid Films* **1996**, *277*, 162–168.
(23) Orilall, M. C.; Abrams, N. M.; Lee, J.; Disalvo, F. J.; Wiesner, U. *J. Am. Chem. Soc.* **2008**, *130*, 8882–8883.
(24) Zumer, M.; Nemanic, V.; Zajec, B.; Remskar, M.; Mrzel, A.; Milhailovic, D. *Appl. Phys. Lett.* **2004**, *84*, 3615.
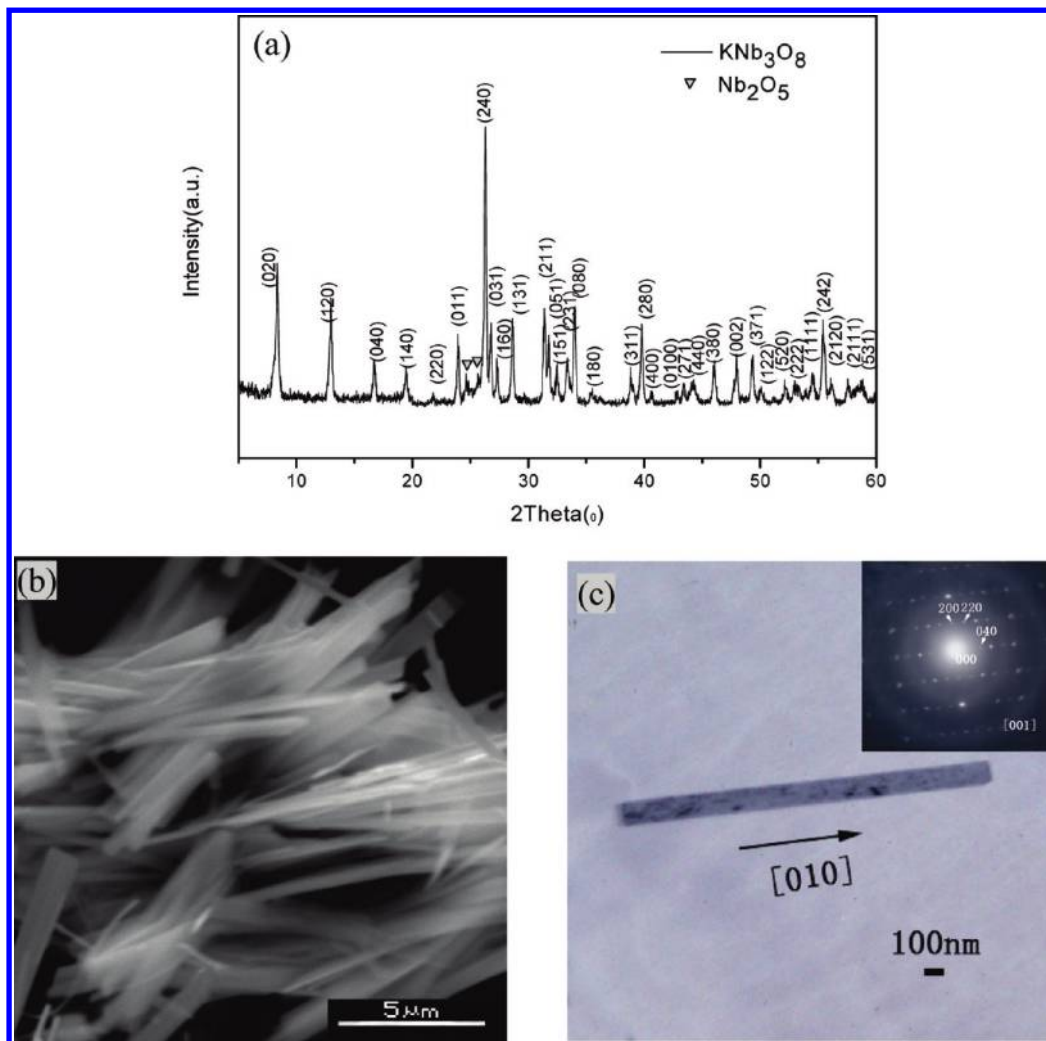(25) Dion M.; Ganne, M.; Tournoux, M. *Mater. Res. Bull.* **1981**, *16*, 1429−1435.

Figure 1. (a) XRD pattern of KNb_3O_8 particles prepared by molten salt synthesized at 800 °C for 3 h and (b) SEM micrograph of the KNb_3O_8 particles. (c) TEM image of the KNb_3O_8 rod with a typical SAED pattern obtained from the rod.

because of its considerable stability, and this quality has raised considerable interest in its use. Previous investigations have shown that the physical properties of Nb_2O_5 depend on the dimensions and shapes of its crystals.[20,24] For example, 1D Nb_2O_5 was an excellent electron field emission emitter with a fairly low turn-on and threshold field,[12] and in our previous work, we reported that rodlike Nb_2O_5, which was obtained from rodlike KNb_3O_8 by a type of topochemical method, could be used as precursor to synthesize rodlike $(Na,K)NbO_3$ with high piezoelectric properties.[26] However, in the previous studies, the investigations of the phase evolution of synthesizing niobium pentaoxides were few. Furthermore, there are many isomeric compounds of the niobium pentaoxide, such as TT− (pseudohexagonal), T− (orthorhombic, *Pbam*), B− (monoclinic), N− (monoclinic, C12/m1), P− (monoclinic), M− (monoclinic), and H−Nb_2O_5 (monoclinic, P2).[27] These different structures have different properties, and it is therefore important to identify these phases and to study the phase evolution during the synthetic process.

We tend to synthesize the T−Nb_2O_5 (a low-temperature form, which can transform to H−Nb_2O_5 at 1000 °C) and H−Nb_2O_5 (a high-temperature form).[27] They are the most common forms among the niobium pentaoxides. Normally, Nb_2O_5 was anomalous (bought from Ningxia Orient Tantalium Industry Co. Ltd.). Here, we report the synthesis via a topochemical method of rodlike (identified to be H−Nb_2O_5) and platelet-like (identified to be T−Nb_2O_5) Nb_2O_5 from rodlike KNb_3O_8 and platelet $K_4Nb_6O_{17}$, respectively. The structure and morphology of the as-prepared $K_4Nb_6O_{17}$, KNb_3O_8, and Nb_2O_5 particles during the synthetic process were investigated. Both rodlike H−Nb_2O_5 and platelet T−Nb_2O_5 were also used as precursors to form $KNbO_3$ with different shapes, in molten salt KCl, and the possible reaction mechanism was discussed.

Experimental Section

Analytical reagent-grade Nb_2O_5 (>99.9%), K_2CO_3 (>99.0%), and KCl (>99.5%) were used as raw materials. To prepare 1D rodlike Nb_2O_5, rodlike precursor KNb_3O_8 was first prepared using the MSS method. K_2CO_3, Nb_2O_5, and KCl were mixed in ethanol according to a molar ratio of 0.1:3:30. The mixture was dried and heated at 800 °C for 3 h. The as-synthesized powders were washed several times with

(26) Li, L. H.; Deng, J.; Chen, J.; Sun, X.; Yu, R.; Liu, G.; Xing, X. *Chem. Mater.* **2009**, *21*, 1207–1213.
(27) Schafer, H.; Gruehn, R.; Schulte, F. *Angew. Chem., Int. Ed.* **1966**, *5*, 40–52.

hot deionized water to remove the remnant KCl molten salts. Then, 1 g of prepared rodlike KNb_3O_8 was added to a 400 mL HNO_3 (2 M) solution and stirred for 48 h at 100 °C. After the products were filtered and rinsed with distilled water, the as-prepared powders were dried in the oven and heated at 600 °C for 1 h to transform into a rodlike Nb_2O_5 powder. As for the synthesis of 2D plate-like Nb_2O_5, $K_4Nb_6O_{17}$ was first prepared using the MSS method. K_2CO_3, Nb_2O_5, and KCl were mixed in ethanol according to a molar ratio of 2:3:10. The dry mixture was heated at 1060 °C for 3 h and then also washed to remove residual KCl salts. Then, 1 g of the as-synthesized plate-like $K_4Nb_6O_{17}$ was added to a 400 mL HNO_3 (2 M) solution and stirred for 7 days at 100 °C. The as-synthesized protonic niobate was filtered and rinsed with distilled water and then heated at predetermined temperatures of 350–750 °C for 1 h to transform into plate-like Nb_2O_5 powder. Finally, $KNbO_3$ particles with different morphologies were synthesized from Nb_2O_5 precursors with different shapes using the MSS method. The ratio of Nb_2O_5/K_2CO_3 was 1:1. The mixtures were heated at 800 °C for 2 h in an equal weight of molten salt KCl. The remnant molten salts were removed from the products with hot deionized water.
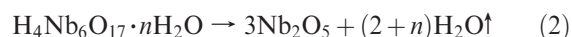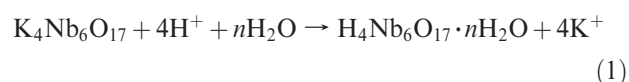
The structure of the samples was characterized by X-ray diffraction patterns (XRD, Model M21XVHF22), and the microstructure of the samples was observed using scanning electron microscopy (SEM, Model CAMBRIDGE S-360). The composition of the powders was determined by energy dispersive X-ray (EDX) analysis in a field-emission scanning electron microscope. Transmission electron microscopy (TEM) observations and the corresponding selected area electron diffraction (SAED) patterns were performed on a transmission electron microscope (model: JEM-100CXII, JEOL, Japan), and the samples were prepared by placing a drop of dilute alcohol to disperse the crystals on a carbon covered copper grid. Raman-scattering data were collected in the frequency range of 100–1100 cm^{-1} using a Raman spectrometer (Model JYT6400, Jobin Yvon, France).

Results and Discussion

KNb_3O_8 was prepared in a KCl melt at 800 °C for 3 h. Figure 1 shows the XRD patterns of the as-synthesized powders. The XRD peaks (see Figure 1a), except for weak peaks at $2\theta = 25–27°$, can be assigned to the orthorhombic phase of KNb_3O_8 (JCPDS 75–2182). The peaks at $2\theta = 25–27°$ can be ascribed to the reflection of the Nb_2O_5 phase (JCPDS number: 37–1468), which is detected as an impure phase. The morphology of the particles (Figure 1b) shows a large amount of rods with diameters of several hundred nanometers and a length of several micrometers. The direction of the KNb_3O_8 rod was along [010], observed from TEM and SAED patterns (see Figure 1c). The rodlike Nb_2O_5 could be obtained by heat treatment of the as-prepared precursor protonic niobate, which was prepared by the proton-exchanged reaction of KNb_3O_8 rods in a HNO_3 solution (2 M). The XRD pattern of the as-prepared protonic niobate could be indexed as orthorhombic $H_3ONb_3O_8$ (JCPDS 44–672, see Figure S1a, Supporting Information). The EDX spectrum shows that the as-prepared protonic niobate does not contain potassium, which confirms the complete conversion from KNb_3O_8 to $H_3ONb_3O_8$ (see Figure S1b, Supporting Information). It was reported that Nb_2O_5 could be formed above 400 °C from $H_3ONb_3O_8$.[28] In our work, niobium pentaoxide rods were achieved (see Figure 2a) by the

heat treatment of $H_3ONb_3O_8$ at 600 °C, which kept the shape and size of the precursors KNb_3O_8. The phase of rodlike niobium oxide was determined to be monoclinic $H-Nb_2O_5$ (JCPDS 37–1468, Figure 2b), and the SAED pattern (inset of Figure 2c) taken from the individual rod shown in Figure 2c described the nature of a single crystal of Nb_2O_5 with the growth direction along [100].

The $K_4Nb_6O_{17}$ sample was prepared by molten salt synthesis at 1060 °C for 3 h. All of the XRD peaks of the sample can be assigned to the perovskite-type $K_4Nb_6O_{17}$ phase (JCPDS 76–977, see Figure 3). Well-developed plate-like layered crystals of $K_4Nb_6O_{17}$ can be seen in Figure 4a. $K_4Nb_6O_{17}$ particles are rectangular platelets with a width of 1–10 μm, a length of 10–20 μm, and a thickness of 0.2–2 μm. The XRD investigation also showed the phase evolution from the as-synthesized platelet protonic niobate (which was obtained from $K_4Nb_6O_{17}$ treated in HNO_3 (2 M) solution during an ion-exchange reaction) to Nb_2O_5 by calcination. The niobium pentaoxide was determined to be orthorhombic $T-Nb_2O_5$ (JCPDS 30–873, Figure 3). The layered structure of $K_4Nb_6O_{17}$ is preserved to the as-prepared platelet protonic niobate, as seen by the (040) reflection at about 11°, a peak typical of the layered structure. The peak at 28° has become the strongest reflection, since it is the (002) reflection from lattice planes contained within one sheet, and other (*hkl*) reflections with two or three nonzero indices have been extinguished in the ion-exchange process. The EDS spectrum also shows that the as-prepared platelet protonic niobate does not contain potassium (see Figure S2, Supporting Information). With the calcined temperature increasing from 500 to 750 °C, the XRD peaks of the prepared particles became stronger and sharper. It indicated that the crystallization of Nb_2O_5 became better. Therefore, via the ion-exchange process, the as-prepared platelet protonic niobate should be $H_4Nb_6O_{17} \cdot nH_2O$, and we assumed the conversion as being

$$K_4Nb_6O_{17} + 4H^+ + nH_2O \rightarrow H_4Nb_6O_{17} \cdot nH_2O + 4K^+ \tag{1}$$

$$H_4Nb_6O_{17} \cdot nH_2O \rightarrow 3Nb_2O_5 + (2+n)H_2O\uparrow \tag{2}$$

The morphology of Nb_2O_5 inherited the $K_4Nb_6O_{17}$ precursor's shape, which also exhibited a plate-like shape (see Figure 4b). The TEM image and SAED pattern of the obtained platelet Nb_2O_5 demonstrated that the platelets were single crystals (see Figure 4c).

Figure 5 shows Raman spectra of KNb_3O_8 and $H_3ONb_3O_8$. It was reported that various niobates with highly distorted NbO_6 units contained short Nb–O bonds and show Raman bands due to a stretching mode around 850–1000 cm^{-1}.[29] From the Raman spectrum of KNb_3O_8, a sharp and strong band was observed at 950 cm^{-1}. This band was assigned to the stretching mode of short Nb–O bonds ($\sim$1.73) of highly distorted NbO_6 units, which stuck out into interlayers, as observed in ref 30. Compared with those of the layered KNb_3O_8, the Raman studies of the $H_3ONb_3O_8$ indicated that the Nb–O terminal bond was affected by a H^+-exchanged reaction, since the Raman band at $\sim$950 cm^{-1}

(28) Nedjar, R.; Borel, M. M.; Raveau, B. *Mater. Res. Bull.* **1985**, *20*, 1291–1296.

(29) Pugh, C.; Percec, V. *Chem. Mater.* **1991**, *3*, 107–115.
(30) Kudo, A.; Sakata, T. *J. Phys. Chem.* **1996**, *100*, 17323–17326.
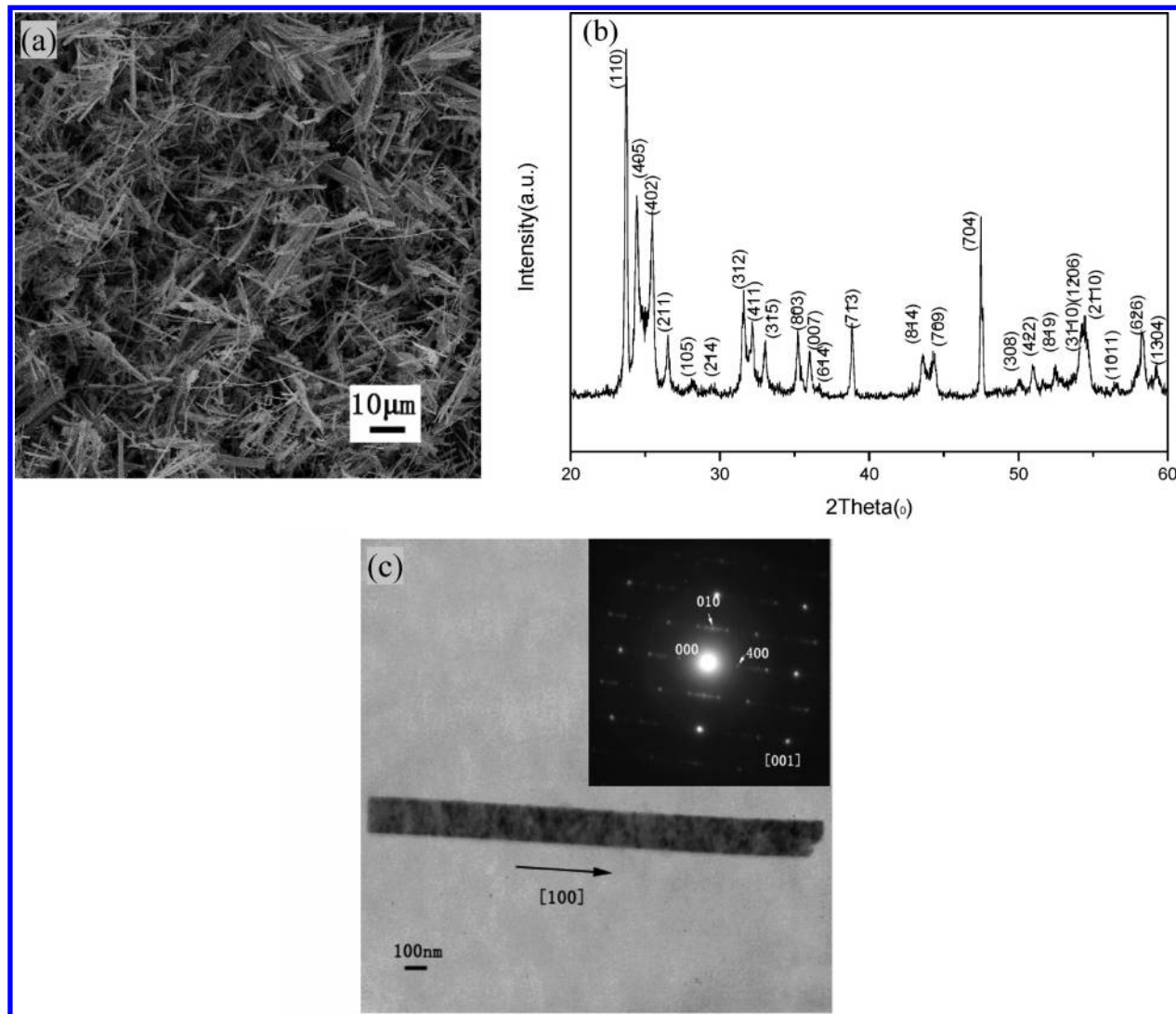
Figure 2. (a) SEM micrograph of the H−Nb$_2$O$_5$ particles. (b) XRD pattern of the H−Nb$_2$O$_5$ particles. (c) TEM image of the H−Nb$_2$O$_5$ rod with a typical SAED pattern obtained from the KNb$_3$O$_8$ rod.
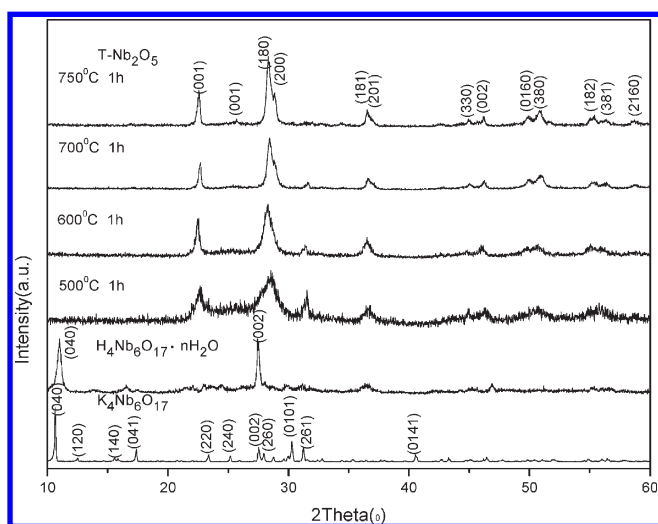

Figure 3. XRD patterns of the transformation from K$_4$Nb$_6$O$_{17}$ to T−Nb$_2$O$_5$.

became weak and broad and a new weak band arose at 974 cm^{-1}. The hydrogen bonds, which were formed by a

H$^+$-exchanged reaction, in the layered oxide H$_3$ONb$_3$O$_8$ structure, associated with the interlayer terminal oxygen atoms of NbO$_6$ to form Nb−O···H bonds. A similar phenomenon was observed in the layer structured HCa$_2$-Nb$_3$O$_{10}$, which was obtained from KCa$_2$Nb$_3$O$_{10}$ by a H$^+$-exchanged reaction.[31] Raman spectra of native and H$^+$-exchanged K$_4$Nb$_6$O$_{17}$ also showed the resemblance discussed above (see Figure 6). As a sharp and strong band was observed at 880 cm^{-1}, K$_4$Nb$_6$O$_{17}$ consisted of highly distorted NbO$_6$ units due to the two-dimensional structure, and the Nb−O bonds which stuck out into interlayers were short.[32] For H$^+$-exchanged K$_4$Nb$_6$O$_{17}$, the intensity of the band was decreased, and a new weak band appeared at 940 cm^{-1}. As the H$_3$O$^+$ ions replaced the K$^+$ ions from layered K$_4$Nb$_6$O$_{17}$, the hydrogen located between the layers of H$^+$-exchanged K$_4$Nb$_6$O$_{17}$ and associated with all of the interlayered terminal oxygens of NbO$_6$ to form Nb−O···H bonds. Therefore, the Raman study of both of H$^+$-exchanged KNb$_3$O$_8$ and K$_4$Nb$_6$O$_{17}$ revealed that hydrogen bonding due to the H$^+$-exchanged reaction resulted in a decrease in

(31) Jehng, J. M.; Wachs, I. E. *Chem. Mater.* **1991**, *3*, 100–107.
(32) Gasperin, M.; Bihan, M. T. L. *J. Solid State Chem.* **1982**, *43*, 346–353.
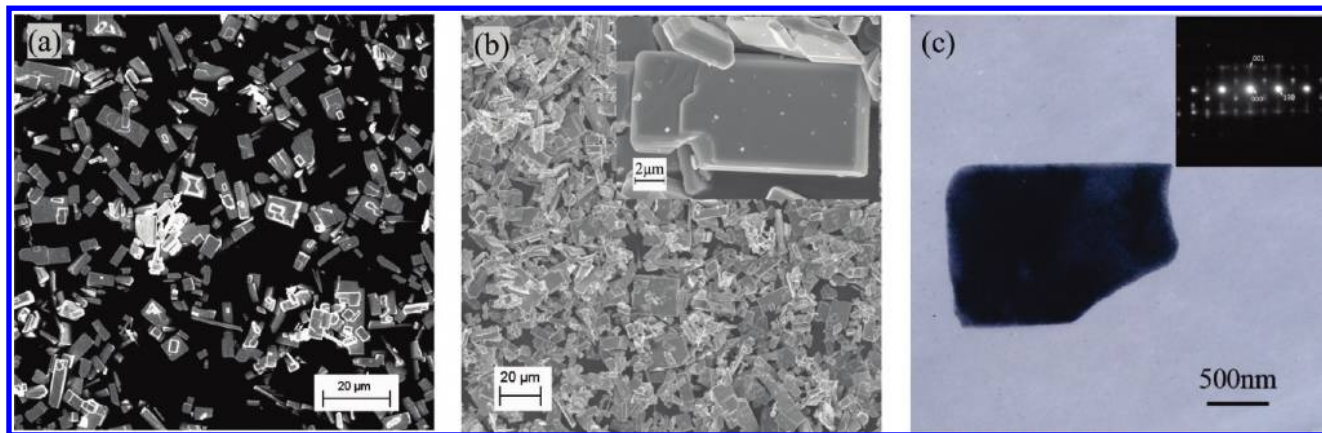
Figure 4. SEM patterns of (a) $K_4Nb_6O_{17}$ and (b) $T-Nb_2O_5$ obtained from $K_4Nb_6O_{17}$; (c) TEM image of the Nb_2O_5 plate with a typical SAED pattern obtained from the plate.

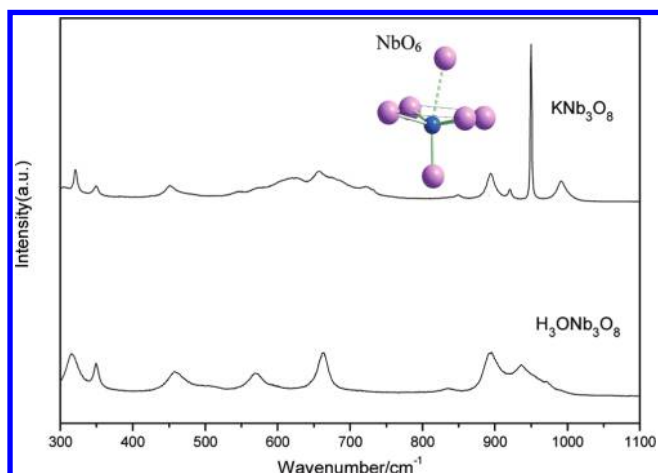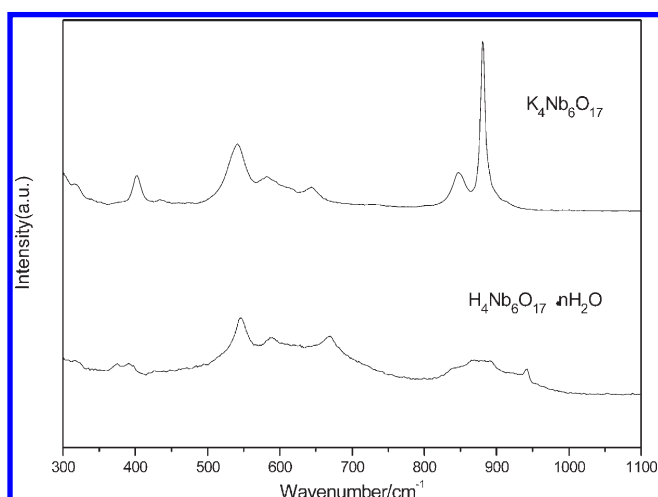**Figure 5.** Raman spectra of KNb_3O_8 and $H_3ONb_3O_8$ particles.

Figure 7. Raman spectra of $H-Nb_2O_5$ and $T-Nb_2O_5$.

Nb–O stretching associated with NbO_6 octahedra and NbO_4 tetrahedra. The corresponding transverse optical modes were observed in the $600-700$ cm^{-1} region. The shoulder peak appearing in this region might be due to anisotropy. The weak bands observed in the $350-560$ cm^{-1} were attributed to be the T_{2g} mode. The strong peaks observed in the range $200-300$ cm^{-1} were assigned to the T_{2u} modes. All of these results revealed the fact that the as-prepared Nb_2O_5 obtained from KNb_3O_8 rods was in the H phase ($H-Nb_2O_5$),[33] in agreement with the results of the XRD experiment. As for the platelet Nb_2O_5, the major band is at 690 cm^{-1}, which is the characteristic band for the structure consisting of NbO_6 and NbO_7 octahedra-sharing corners.[34] The platelet Nb_2O_5 spectrum was assigned to be $T-Nb_2O_5$, which was consistent with that of $T-Nb_2O_5$ reported in the literature,[35] and it was also in agreement with the results of the XRD measurement.

The phase evolution from KNb_3O_8 to $H-Nb_2O_5$ and $K_4Nb_6O_{17}$ to $T-Nb_2O_5$ can be also interpreted in terms of the structures involved. The structures[33,36] of KNb_3O_8,

Figure 6. Raman spectra of native and H^+-exchanged $K_4Nb_6O_{17}$.

the Nb–O bond order and its corresponding vibrational frequency.

The Raman spectra of the as-grown Nb_2O_5 rods, obtained from KNb_3O_8 and Nb_2O_5 platelets from $K_4Nb_6O_{17}$, are exhibited in Figure 7. As for the Raman spectrum of Nb_2O_5 rods, the bands observed in the $700-1000$ cm^{-1} region correspond to the longitudinal optical modes of the
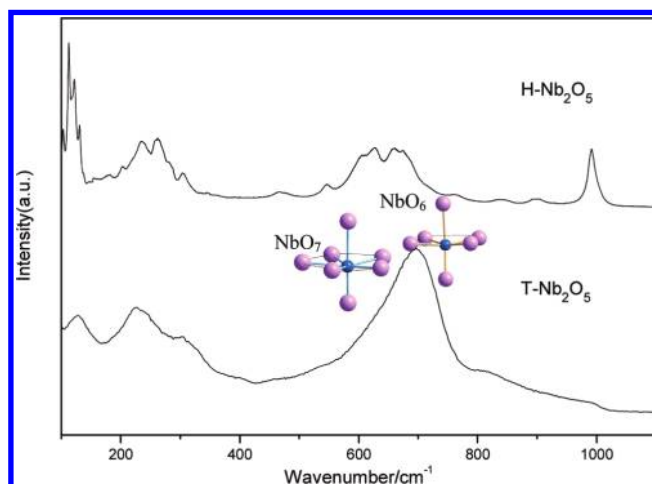
(33) Mcconnell, A. A. *Spectrochim. Acta* **1976**, *32A*, 1067–1976.
(34) Blasse, G.; Van den Heuvel, G. P. M. *Mater. Res. Bull.* **1972**, *7*, 1041–1043.
(35) Jehng, J. M.; Wachs, I. E. *Catal. Today* **1990**, *8*, 37–55.
(36) (a) Gasperin, P. M. *Acta Crystallogr.* **1982**, *B38*, 2024–2026. (b) Gasperin, M.; le Bihan, M. T. *J. Solid State Chem.* **1982**, *43*, 346–353. (c) Katsuo, K. *Acta Crystallogr.* **1976**, *B32*, 764–767.
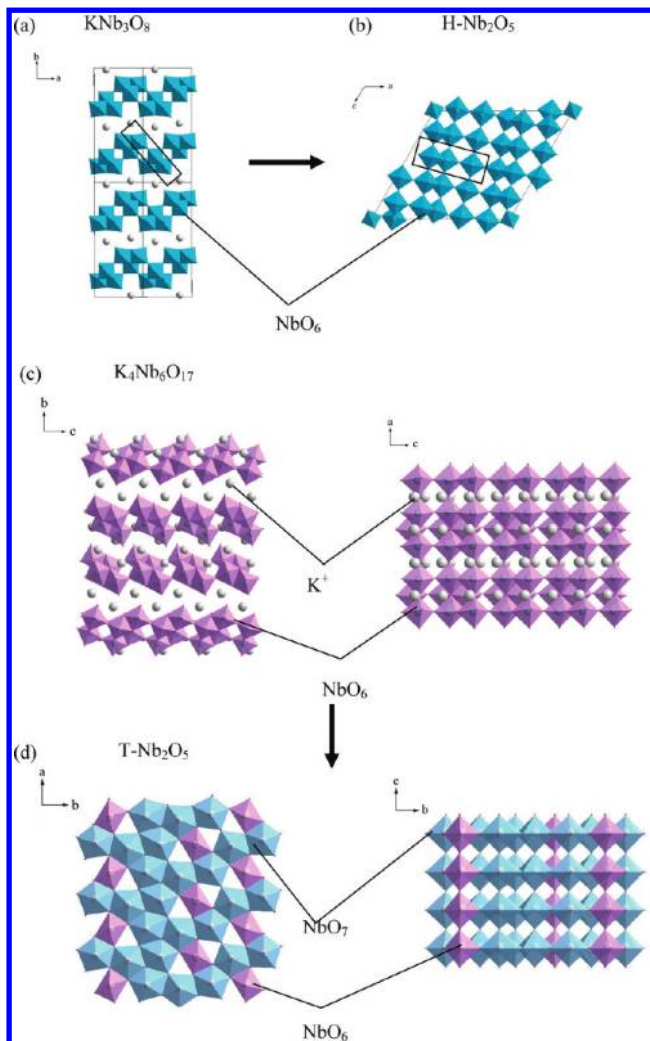
Figure 8. Crystal structures of (a) KNb_3O_8, (b) $H-Nb_2O_5$, (c) $K_4Nb_6O_{17}$, and (d) $T-Nb_2O_5$.

$H-Nb_2O_5$, $K_4Nb_6O_{17}$, and $T-Nb_2O_5$ are shown in Figure 8. The structure of KNb_3O_8 can be characterized as a stacking of $-Nb_3O_8-$ sheets consisting of corner-sharing and edge-sharing NbO_6 octahedra, and K^+ atoms located between the $-Nb_3O_8-$ sheets. In each sheet, three NbO_6 octahedra connect by sharing corners and edges along the [001] direction. Our XRD patterns and Raman spectra study showed that H_3O^+ tended to take the place of K^+ between the $-Nb_3O_8-$ sheets to form $Nb-O\cdots H$ and found the structure of $H_3ONb_3O_8$ to be similar to that of KNb_3O_8.[28] Both the structures KNb_3O_8 and Nb_2O_5 could be described as being built up from identical units of three octahedra with corner and edge sharing shown in the oblong loop (Figure 8a,b). This interpretation explains the fact that the transformation from KNb_3O_8 to Nb_2O_5 is a soft reaction. First, H_3O^+ exchanges the K^+ from $-Nb_3O_8-$ sheets during the proton-exchanged reaction. Then, after heat treatment, H_2O is eliminated from the $-Nb_3O_8-$ sheets, and the sheets became closer and connected with the NbO_6 octahedra sharing the corners. So the shape of Nb_2O_5 does not change much from that of KNb_3O_8, which corresponds to the morphology of $H-Nb_2O_5$, and this can explain why the $H-Nb_2O_5$ is crystalline, as observed from the SAED pattern.

The structure, viewed along the a axis of the orthorhombic cell, is composed of layers of edge-sharing NbO_6 octahedra, with the K^+ ions located between the layers (see Figure 8c). The octahedra share corners in the direction of the a axis. The structure of $T-Nb_2O_5$ is shown in Figure 8d. Edge-sharing NbO_6 and NbO_7 units are parallel to the ab plane. These are linked by corner-sharing polyhedra along the c axis to form the three-dimensional structure. The transformation from $K_4Nb_6O_{17}$ to $T-Nb_2O_5$ is similar to that of KNb_3O_8 to $H-Nb_2O_5$. During the proton exchange reaction, H_3O^+ ions exchange the K^+ ions from $K_4Nb_6O_{17}$ layers. When the temperature is increased, the H_2O molecules evaporate, and the layers become closer. There are more K^+ ions in the $K_4Nb_6O_{17}$ layers than in the KNb_3O_8 layers. Therefore, more H_2O is eliminated from H^+-exchanged $K_4Nb_6O_{17}$ layers, and this causes the formation of edge-sharing NbO_7 units formed in $T-Nb_2O_5$. Close examination of the structure reveals that, along one dimension of both of $K_4Nb_6O_{17}$ (along [100]) and $T-Nb_2O_5$ (along [001]), the polyhedra are corner-sharing, and along other dimensions of $K_4Nb_6O_{17}$ (along [001]) and $T-Nb_2O_5$ (along [010]), the polyhedra are alternatively corner-sharing and edge-sharing. This may be the reason why the shape of $T-Nb_2O_5$ does not change much from that of $K_4Nb_6O_{17}$, and why $T-Nb_2O_5$ particles are single crystals, as observed from the SAED pattern. Hence, we may conclude that both the rodlike KNb_3O_8 and platelet $K_4Nb_6O_{17}$ are first synthesized with the MSS method, and then the conversions from KNb_3O_8 to $H-Nb_2O_5$ and $K_4Nb_6O_{17}$ to $T-Nb_2O_5$ are done with the topochemical method. The topochemical method, associated with the use of localized solid-state compound transformations via the exchange, deletion, or insertion of individual atoms,[37] is therefore one of the strategic approaches aimed at controlling material synthesis. On the other hand, the MSS method represents a rapid and large-scale synthesis of oxides, allowing one to control the morphology of powder samples.[38,39] Consequently, the combination of the two methods is the effective approach in the preparation of oxides with special morphology.

It was expected that high-anisotropic niobium oxides were suitable to be templates to generate 1D or 2D structures of oxides. To confirm this, low-dimension $KNbO_3$ particles were synthesized with the MSS method in KCl salt at 800 °C for 2 h by using different precursors, the as-prepared rodlike and platelet Nb_2O_5 with equal molar K_2CO_3, respectively. The XRD patterns (Figures S3a and S4a, Supporting Information) confirmed that both of the synthesized pure $KNbO_3$ products were orthorhombic (JCPDS 71−946). $KNbO_3$ rods with a diameter of several hundred nanometers and a length of several micrometers were observed in Figure S3b (Supporting Information), and $KNbO_3$ plates with a width of 1−10 μm, a length of 10−20 μm, and a thickness of 0.2−2 μm were found (see Figure S4b, Supporting Information). Both the rodlike and platelet $KNbO_3$ retained the shape of their precursors. This phenomenon could be explained by a "template formation" mechanism.[40] Among
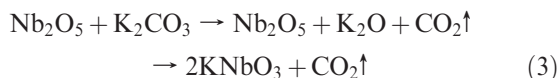
(37) Schaak, R. E.; Mallouk, T. E. *Chem. Mater.* **2002**, *14*, 1455–1471.
(38) Chen, J.; Xing, X.; Watson, A.; Wang, W.; Yu, R.; Deng, J.; Yan, L.; Sun, C.; Chen, X. *Chem. Mater.* **2007**, *19*, 3598–3600.
(39) Cai, Z.; Xing, X.; Yu, R.; Sun, X.; Liu, G. *Inorg. Chem.* **2007**, *46*, 7423–7427.
(40) Xu, C. Y.; Zhang, Q.; Zhang, H.; Zhen, L.; Tang, J.; Qin, L. C. *J. Am. Chem. Soc.* **2005**, *127*, 11584–11585.

various niobium oxides, niobium pentaoxide (Nb_2O_5) is the thermodynamically most stable phase.[41] In this study, H− and T−Nb_2O_5 showed good stability in molten salt and almost did not dissolve in KCl, while K_2O is much more soluble than Nb_2O_5 in KCl. (K_2O primarily dissolved into the salt and diffused onto the surfaces of Nb_2O_5.) The reactions are described as follows:

$$Nb_2O_5 + K_2CO_3 \rightarrow Nb_2O_5 + K_2O + CO_2\uparrow$$
$$\rightarrow 2KNbO_3 + CO_2\uparrow \qquad (3)$$

Since $KNbO_3$ can well retain the morphology of Nb_2O_5, it is also expected that the highly anisotropic, stable H−Nb_2O_5 and T−Nb_2O_5 can be used to synthesize other highly anisotropic niobate, which possesses high piezoelectricity for their anisotropism, such as rodlike and platelet $(Na,K)NbO_3$. In addition, they are also suitable to be used as seeds for the preparation of texture niobate ceramics. Furthermore, rodlike Nb_2O_5 may be used as the electron field emission emitters, and further study is needed.

Conclusion

Rodlike H−Nb_2O_5 and platelet T−Nb_2O_5 single crystals were synthesized by the topochemical method from rodlike KNb_3O_8 and platelet $K_4Nb_6O_{17}$, which were in turn

(41) Varghese, B.; Haur, S. C.; Lim, C. *J. Phys. Chem. C* **2008**, *112*, 10008–10012.

prepared by the MSS method. Raman spectrogram studies combined with XRD and SEM/TEM measurements revealed that the structure of H−Nb_2O_5 was similar to that of KNb_3O_8, and the structure of T−Nb_2O_5 to that of $K_4Nb_6O_{17}$, so both of the rodlike and platelet shapes of Nb_2O_5 could well retain that of their precursors. Using the MSS method, rodlike and platelet $KNbO_3$ were derived from stable H−Nb_2O_5 and T−Nb_2O_5. It is reasonable to expect that this kind of low-dimension Nb_2O_5 could be used to synthesize other highly anisotropic niobate, and this type of topochemical method combined with MSS could be suitable to synthesize other kinds of oxides with other specialized shapes.

Supporting Information Available: XRD and EDX of $H_3ONb_3O_8$ particles obtained from rodlike KNb_3O_8 particles; EDX pattern of $H_4Nb_6O_{17} \cdot H_2O$ particles obtained from platelet $K_4Nb_6O_{17}$ particles; XRD and SEM of the rodlike $KNbO_3$ particles obtained from rodlike precursor H−Nb_2O_5; XRD and SEM of the platelet $KNbO_3$ particles obtained from platelet precursor T−Nb_2O_5. This material is available free of charge via the Internet at http://pubs.acs.org.